Check for updates

How to cite: *Angew. Chem. Int. Ed.* **2020**, *59*, 16527–16535
International Edition: doi.org/10.1002/anie.202003695
German Edition: doi.org/10.1002/ange.202003695

Oxidative Dehydrogenation | Hot Paper

Why Boron Nitride is such a Selective Catalyst for the Oxidative Dehydrogenation of Propane

Juan M. Venegas[+], Zisheng Zhang[+], Theodore O. Agbi, William P. McDermott, Anastassia Alexandrova, and Ive Hermans**

Abstract: *Boron-containing materials, and in particular boron nitride, have recently been identified as highly selective catalysts for the oxidative dehydrogenation of alkanes such as propane. To date, no mechanism exists that can explain both the unprecedented selectivity, the observed surface oxyfunctionalization, and the peculiar kinetic features of this reaction. We combine catalytic activity measurements with quantum chemical calculations to put forward a bold new hypothesis. We argue that the remarkable product distribution can be rationalized by a combination of surface-mediated formation of radicals over metastable sites, and their sequential propagation in the gas phase. Based on known radical propagation steps, we quantitatively describe the oxygen pressure-dependent relative formation of the main product propylene and by-product ethylene. Free radical intermediates most likely differentiate this catalytic system from less selective vanadium-based catalysts.*

Introduction

Hexagonal boron nitride (hBN) and other boron-containing materials recently emerged as promising catalysts for the oxidative dehydrogenation (ODH) of small alkanes, with unprecedented high olefin selectivity.[1–6] Breakthroughs in ODH research could drastically reduce the energy that is required in the synthesis of building block olefins. It has been shown that the oxidation of the catalyst surface to an amorphous boron hydroxy oxide layer is crucial for ODH activity, and the surface composition of these boron-based materials is highly dynamic and sensitive to the reaction conditions.[7–9] As more information is obtained from these complex materials, it is imperative to continuously revisit mechanistic hypotheses to support experimental evidence. For example, initial mechanisms that rationalized the reactivity of boron nitride during ODH had to be updated to account for the reactivity of other boron-containing materials, such as B_4C, NiB_2, and amorphous boron.[1]

Along these lines, studies on supported boron oxide catalysts have presented a mechanistic hypothesis for the ODH of propane featuring BO_3 and BO–H species.[10] While compelling because of its use of thermodynamically stable BO_3 units assembled into boroxol rings, the mechanism fails to explain ODH reaction kinetics and material characterization evidence. The proposed reaction sequence with a rate-determining H abstraction of BO–H by O_2 would lead to a first-order dependence on O_2 concentration and zero-order dependence on propane—neither of which are supported by experimental studies from various groups.[4,5,11,12] Furthermore, spectroscopic characterization of supported B/SiO_2 does indeed show the presence of boroxol rings prior to ODH, but these motifs are no longer present in the surface after carrying out ODH chemistry.[8] In a targeted study of isolated BO_3 species for ODH, it was recently demonstrated that an MWW zeolite with isolated BO_3 units incorporated into its framework is inactive for propane activation.[13] In contrast, BO_x clusters supported on silica demonstrate catalytic activity.[8] These gaps, and often contradictions, in knowledge on the ODH reaction mechanism highlight the need to consider additional surface species to rationalize the performance of boron-based ODH catalysts. The dynamic surface changes during ODH may benefit from computational investigations of metastable surface sites, beyond thermodynamically stable species such as BO_3. This approach is a key focus of the present report.

Beyond surface speciation, there are observations from catalytic studies that require complementary investigation. Reaction kinetic studies have shown that the predominance of dehydrogenation versus C–C bond cleavage—the most important side-reaction—is controlled by the oxygen concentration.[11,14] To rationalize these observations, we explored the possible role of gas-phase chemistry and found strong experimental indications of surface-initiated gas-phase radical reactions. It was observed, for instance, that the ODH reactivity scales with total packed bed volume rather than the

[*] Dr. J. M. Venegas,[+] T. O. Agbi, Prof. Dr. I. Hermans
Department of Chemical and Biological Engineering
University of Wisconsin—Madison
1415 Engineering Drive, Madison, WI 53706 (USA)
E-mail: hermans@chem.wisc.edu
Z. Zhang,[+] Prof. Dr. A. Alexandrova
Department of Chemistry and Biochemistry
University of California, Los Angeles
607 Charles E. Young Drive, Los Angeles, CA 90095 (USA)
E-mail: ana@chem.ucla.edu
W. P. McDermott, Prof. Dr. I. Hermans
Department of Chemistry
University of Wisconsin—Madison
1101 University Avenue, Madison, WI 53706 (USA)
Dr. J. M. Venegas[+]
Present address: Performance Silicones Process R&D
The Dow Chemical Company
2651 W. Salzburg Road, Midland, MI 48640 (USA)
[+] These authors contributed equally to this work.
Supporting information and the ORCID identification number(s) for the author(s) of this article can be found under: https://doi.org/10.1002/anie.202003695.

 © 2020 Wiley-VCH Verlag GmbH & Co. KGaA, Weinheim

hBN mass only, and that for a given bed volume the reaction rate features a maximum as a function of the hBN loading.[15] These observations are at odds with a pure surface-catalyzed reaction but rather suggest a free-radical-mediated mechanism that can be both initiated and quenched by catalytic species.[16] Recently, Zhang, et al. successfully detected radicals during the ODH of propane over hBN catalysts via synchrotron vacuum ultraviolet photoionization mass spectroscopy (SVUV-PIMS), in support of this hypothesis.[17]

Considering the possible radical pathways involved in hBN-catalyzed ODH, we aim to gain insight into the reactions that could take place both at the surface and in the gas phase. Additionally, the role of H_2O has not been extensively explored to date, despite it being a significant reaction product and literature precedent suggesting its possible synergistic role in improving oxidation performance.[18,19] Gas-phase alkane oxidation chemistry features complex radical-based reaction networks, and this contribution extracts the key features of these reaction mechanisms to explain the unique performance of boron-based ODH catalysts.

Results and Discussion

Steam enhances the ODH activity for boron nitride

Initially, we investigated the difference in reactivity of hBN under standard "dry" conditions (without water added to the reaction feed) and under "wet" conditions (where 10% water vapor was cofed). All experimental details can be found in the Supporting Information. Figure 1 shows the rate dependence on C_3H_8 during ODH under dry and wet conditions at a constant total flow of 50 $mL_{STP}\,min^{-1}$ and differential propane conversions ($X < 10\%$). Under both feed conditions we observed an apparent order 2.1 ± 0.1 in propane, with the wet stream leading to higher reaction rates at all C_3H_8 concentrations. This observed rate-enhancement stands in strong contrast to the inhibiting effect of water that has been reported for supported vanadium ODH catalysts.[20,21]

If the observed increase in reactivity upon addition of steam were due to alkane conversion by new reaction pathways, we would expect differences in conversion–selectivity trends between dry and wet conditions. Instead, Figure 2 indicates that the selectivity towards C_3H_6, at a given conversion, is independent on the addition of steam. It appears then, that the addition of water enhances the rates of pathways already present under standard conditions. To complement these observed activity improvements with wet ODH feeds, we varied water concentrations between 1–20 mol% under two propane concentrations (15 and 25 mol%; Supporting Information, Figure S1). These experiments show a linear increase in propane consumption rates with water content, suggesting water is indeed involved in the formation of reactive species during ODH.

The second-order rate-dependence on C_3H_8 has been a characteristic feature of boron-catalyzed ODH.[1,3] This nonlinear dependence can be explained within the context of a mixed surface–gas-phase mechanism. When using MgO-based catalysts, Leveles et al. hypothesized that the gas-phase contribution to propane conversion can be neglected at low alkane concentrations, relative to surface reactions.[22] Under alkane-rich feeds, however, gas-phase radical chemistry leading to propane H abstraction becomes comparable to surface-mediated propane activation in its contribution to the overall ODH activity. Herein, the rate enhancement observed upon

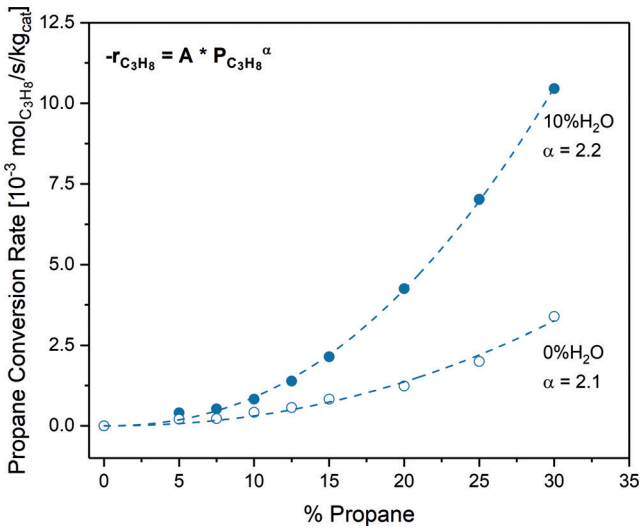

Figure 1. Propane conversion rate as a function of propane concentration with water cofeed (solid symbols) and under standard feed conditions (open symbols). Reaction conditions: $T = 525\,°C$, $F_{total} = 50\ mL_{STP}\,min^{-1}$. Feed composition: 15% O_2, 5–30% C_3H_8, balance N_2. During water cofeed, N_2 flow rates were adjusted to obtain 10% H_2O concentration. α denotes the exponent used to obtain the fitted curve from the power law equation $-r_{C_3H_8} = A\,P_{O_2}{}^{\alpha}$.

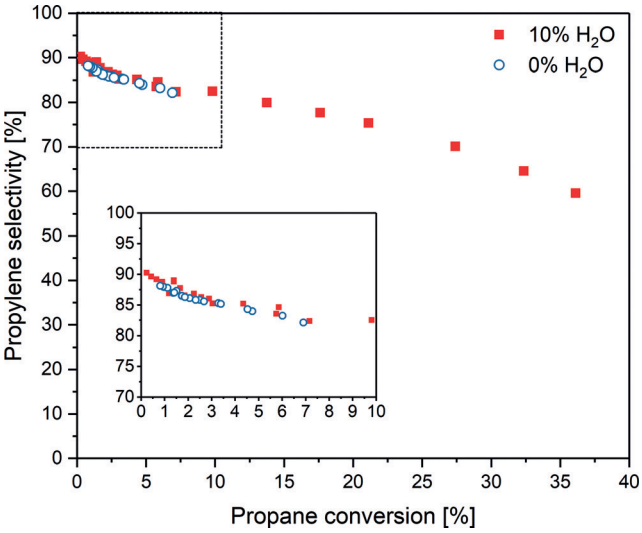

Figure 2. Propylene selectivity as a function of propane conversion during water cofeeding (red symbols) and under standard feed conditions (open blue symbols). Inset: conversions below 10%. Reaction conditions: $T = 525\,°C$, F_{total} flow = 20–80 $mL_{STP}\,min^{-1}$. Feed composition: 15% O_2, 5–30% C_3H_8, balance N_2. During water cofeeding, N_2 flow rates were adjusted to obtain 10% H_2O concentration.

 © 2020 Wiley-VCH Verlag GmbH & Co. KGaA, Weinheim

cofeeding of steam indicates that water may be involved in formation of intermediates that react in the gas phase.

After establishing the synergistic role of water in ODH, we studied the reversibility of its rate-enhancement by cycling "dry" and "wet" conditions over a period of approximately 4 days. During a cycle, the catalyst was exposed to either wet or dry streams (using a 6-way valve to switch streams with minimal flow disturbance) for 12 hours. If irreversible structural changes were to occur due to the presence of added steam, we hypothesize that the steady-state reactivity of the catalyst would evolve with time. For example, if water-induced surface modifications irreversibly lead to more active sites, we would expect steady-state reactivity under dry conditions to increase at a given flow condition. And vice versa, the inhibition of surface species would decrease reactivity, as previously observed for supported vanadium catalysts.[20,21] If the effect of H_2O were only to alter the gas-phase radical concentration, or if surface changes are reversible, the reactivity at each cycle would remain constant during the experiment. Figure 3 reveals that, during the 12 hour cycling periods, the propane conversion steadily increases (during a wet cycle) or decreases (during a dry cycle). However, the asymptotic conversion reached during all cycles remains constant at about 2–3% under dry conditions, and approximately 9–10% during wet feed cycles. Additionally, the observed propylene selectivity during each cycle also remains constant at 85% and 80% during dry and wet cycles, respectively, consistent with the difference in conversion (the full product distribution under each condition is provided in Figure S2).

The cycling experiment may provide insights into the various effects that water has on the observed reactivity. Approximately 70% of the total conversion change happens within the first hour of a cycle. The remaining conversion change occurs throughout the remaining time of the cycle, about 11 hours. These different time scales suggest that water influences the observed reactivity by multiple routes. The high reactivity of radicals suggests that the rapid conversion change may be due to the formation or disappearance of a radical source. As the only difference between cycles is the addition of water, we hypothesize that these radicals stem from the activation of H_2O. The second role of water, which leads to the slower change in propane conversion, is unlikely to involve radicals. This longer time scale effect may involve changes in the concentration of active surface species. This role is supported by the constant conversion–selectivity trends in Figure 2, indicating that no new reaction pathways are enabled. As such, a remaining possibility lies in changes in the concentration of active surface species.

After establishing the reversible nature of water's effect on ODH activity, we assessed whether water may be directly involved in C_3H_8 conversion via an oxygen cutoff experiment (Figure 4). In this test, we performed ODH under wet conditions until stable propane conversion was observed, and oxygen was subsequently removed from the reaction feed. Within the timescale of our GC analysis (that is, ca. 25 min), we observed a complete loss of catalytic activity under anaerobic conditions. This experiment indicates that oxygen-derived intermediates are necessary to form reactive species from H_2O. These observations remind us of the work by Takanabe and Iglesia that suggests chemisorption and activation of O_2 is necessary for the subsequent activation of CH_4 and H_2O under wet oxidative coupling of methane (OCM) over a $Mn/Na_2WO_4/SiO_2$ catalyst.[18]

Oxygen is not only required to observe activity, but its concentration also determines the selectivity during ODH (for changes in product distribution at varying oxygen feed concentrations, see Figure S3). In line with previous reports,[5,11] C–C cracking pathways to produce C_2H_4 become increasingly important under oxygen lean conditions. These trends hold using both dry and wet ODH feeds, highlighting

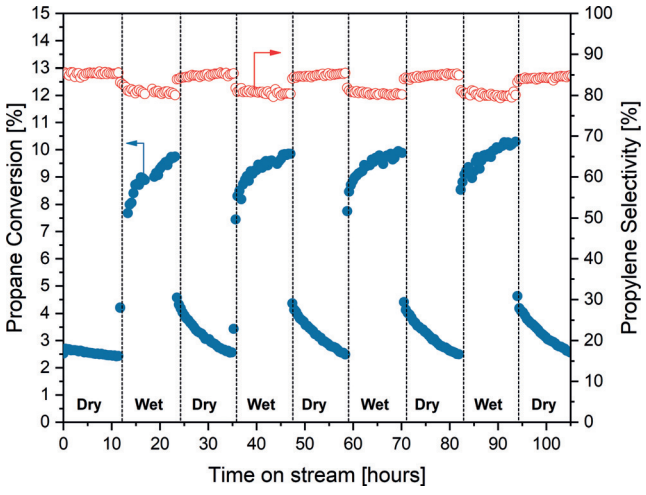

Figure 3. Propane conversion (blue symbols, left axis) and propylene selectivity (red symbols, right axis) as a function of time-on-stream during 12 h cycles of "wet" or "dry" ODH feed. Prior to cycling, the catalyst had undergone ODH under wet conditions for 24 h, and subsequently ODH under dry conditions for 24 h. $T = 525\,°C$, $F_{total} = 40\ mL_{STP}\,min^{-1}$. Dry feed: 30% C_3H_8, 15% O_2, 55% N_2. Wet feed: 30% C_3H_8, 15% O_2, 45% N_2, 10% H_2O.

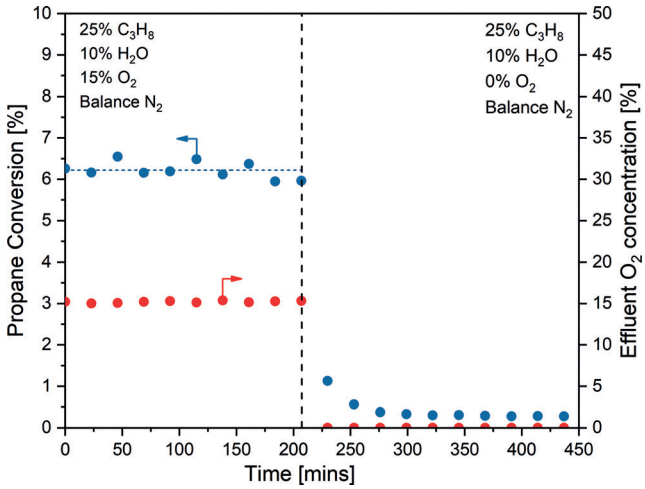

Figure 4. Oxygen cut-off experiment. ODH under a wet reaction feed was run for about 200 min, after which O_2 was removed from the feed and the resulting catalytic activity was monitored. Blue symbols represent observed propane conversion (left axis) and red symbols represent oxygen concentration as determined by GC (right axis).

 © 2020 Wiley-VCH Verlag GmbH & Co. KGaA, Weinheim

once again the possible role of water in enhancing reaction rates already present rather than enabling new reaction pathways. In the context of a surface-mediated gas-phase reaction network, the types of radicals formed may provide rationale behind these observed selectivity trends, as discussed in the proceeding text.

Computational insights

Our previous experimental studies show that the surface of boron-based catalysts oxyfunctionalizes during ODH chemistry, but it remained unclear as to which species in the amorphous hydroxy oxide layer could be responsible for the observed activity.[7,8] The fact that site-isolated BO_3 species with saturated and fully oxidized local environments—as created in a zeolite matrix (that is, B-MWW)—are inactive for ODH suggests that the amorphous hydroxy oxide network is actually key.[13] This hypothesis is further supported by the fact that impregnation of boron onto the inactive B-MWW resulted in an active catalyst (B/B-MWW) featuring B–O–B connectivity.[13] We emphasize that this amorphous interface is highly dynamic and, as such, it is a suspect for presenting metastable active sites. Metastable species may remain a minority, and thus be poorly detectable even by operando characterization.[23,24] Such active sites may be studied by leveraging computational tools. Previous theoretical work reveals a dynamic BO_x surface that does indeed contain metastable surface states with distinct geometries, stoichiometries, and chemistries, which can form on a timescale of picoseconds and become only significantly populated as the temperature is increased from 298 K to 763 K, based on grand canonical simulations.[9] After ruling out the BO_3-type surface units, we obtained three other types of sites that have $>5\,\%$ population at the reaction temperature; all of them contain unsaturated B-B-B units in which the middle B is buried in the sublayer while two ends are exposed (denoted as {BB}). These sites (Figure 5) can be found in the global minimum of the B_5O_2 phase (B_5O_2#1), and the second and third local minimum of the B_6O_3 phase (B_6O_3#2 and B_6O_3#3). The calculated Bader charges of these species (Figure 5) show distinct electronic environments compared to BN_3 or BO_3 (Bader charge: +2.2), which suggests unusual chemical reactivities.

As oxygen is critical to ODH, we first explored a possible route to O_2 activation on {BB} surface species. O_2 chemisorption on {BB} is thermodynamically favorable for all three surface states, and forms barrierless peroxo-like >BO–OB< species. The >BO–OB< cleavage was then explored in B_6O_3#2, B_6O_3#3, and B_5O_2#1. Figure 6 shows the facile O–O bond cleavage (energy barrier of only 49 kJ mol^{-1}) to form >B–O$^{\bullet}$ surface species in B_6O_3#2. This reaction path is similar to those proposed by Aparicio et al. during OCM with Li-doped MgO catalysts, with the formed MO$^{\bullet}$ abstracting H atoms from methane.[25] As expected, the formed BO$^{\bullet}$ species depicted in Figure 6 are highly reactive, readily forming both *i*-propyl (barrierless) and *n*-propyl (5.3 kJ mol^{-1} barrier) radicals from propane, plus BOH surface groups (Figure S4). However, B_6O_3#3 and B_5O_2#1 are further oxidized upon cleavage of >BO–OB< by rapidly interacting with proximate B atoms, and therefore do not produce stable BO$^{\bullet}$ sites.

In parallel to the formation of propyl radicals via the activation of O_2 (Figure S4), we also set out to understand the effect of water. We first investigated how water may interact with the catalyst surface (Figure S5), and the three surface states show very similar behaviors. Upon interaction of water with a {BB} site, the O–H bond in water is lengthened by interactions with a proximate B atom. The calculated transition state related to O–H bond breaking has a barrier of 57, 66, and 89 kJ mol^{-1}, for B_6O_3#2, B_6O_3#3, and B_5O_2#1, respectively. At this point, the B where water adsorption took place adopts the BO_3 geometry and is repelled away from the newly formed BH species, with an overall ΔG of −251, −199, and −123 kJ mol^{-1} for B_6O_3#2, B_6O_3#3, and B_5O_2#1, respectively.

While valuable to assess the role of water under ODH conditions, the predicted pathways do not lead to BO_x species. The >BH species does not appear to be reactive for H abstraction, and our oxygen cutoff experiment (Figure 4) suggests that, under wet conditions, propane conversion still requires the presence of oxygen. The likely fate of the formed B–H species is therefore the reaction with O_2 to form HOO$^{\bullet}$

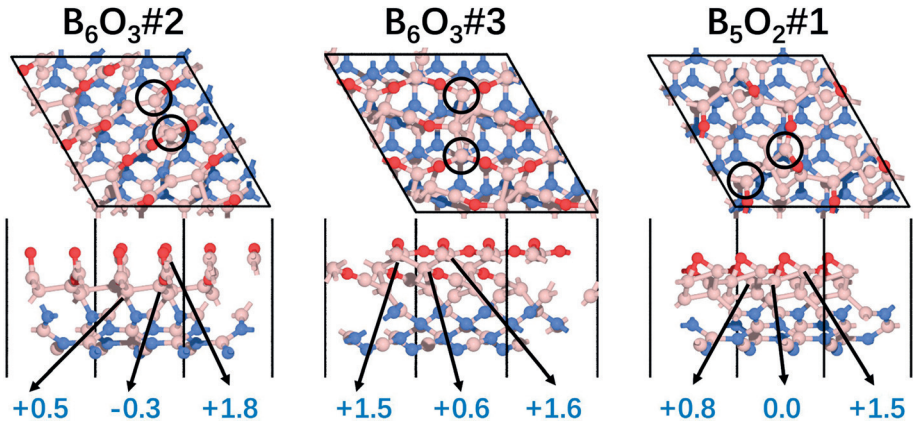

Figure 5. Top and side views of the three surface states studied herein: B_6O_3#2, B_6O_3#3, and B_5O_2#1. The Bader charge of key atoms in the {BB} motif is labeled under the side view of each surface state in blue text. Key: boron (pink), nitrogen (blue), oxygen (red).

 © 2020 Wiley-VCH Verlag GmbH & Co. KGaA, Weinheim

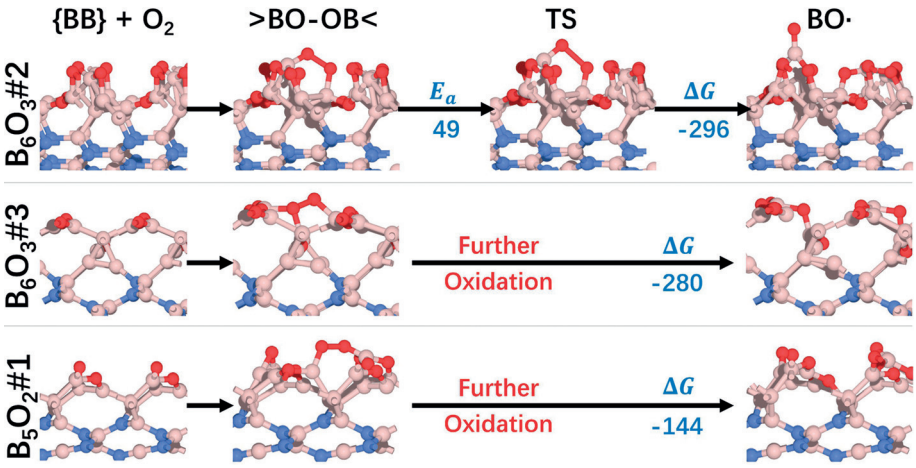

Figure 6. Structural models showing O_2 chemisorption and activation on B_6O_3#2, B_6O_3#3, and B_5O_2#1. The chemisorption steps are all barrierless. The activation energy and overall ΔG values (in kJ mol^{-1}) are labeled on connecting arrows. Key: boron (pink), nitrogen (blue), oxygen (red), hydrogen (white), transition state (TS).

radicals (Reaction (1)). These HOO· radicals subsequently abstract H atoms from the propane substrate, leading to more propyl radicals.

$$BH + O_2 \rightleftharpoons B + HOO\cdot \quad (1)$$

Our calculations show that only B_6O_3#2 can achieve such a reaction, and the predicted pathway for O_2 interaction with >BH in B_6O_3#2 is shown in Figure 7a. This reaction has a computed barrier of 90 kJ mol^{-1} and an overall $\Delta G = -33$ kJ mol^{-1}. As such, surface sites derived from water activation still require O_2 to form the species capable of H abstraction from propane in the gas phase. This readily explains why the catalyst shows no dehydrogenation activity and is only active for ODH.

From the aforementioned exploration of the elemental steps on three potential "hot" active sites, we find that all of them can contribute to the whole map of catalysis to some extent. B_6O_3#2 stands out as the candidate that can chemisorb and activate O_2 into stable BO· to abstract a H atom from propane, as well as activate water into B–H that can react with O_2 to form a free HOO· radical. The barrier for water dissociation in B_6O_3#2 is also lower than those in B_6O_3#3 and B_5O_2#1, suggesting B_6O_3#2 may be the main contributor to water activation.

The properties of B_6O_3#2 can be attributed to the electronic structure of B in the {BB} motif, and its unique geometry (Figure 5). The middle B atom in the {BB} of B_6O_3#2 features an unusual Bader charge of −0.3, suggesting a higher electron density than those in B_6O_3#3 (Bader charge: +0.6) and B_5O_2#1 (Bader charge: 0.0). Moreover, in B_6O_3#2 the top-layer B and O atoms are arranged into chains of B_4O_2 units while the sublayers are relatively rigid, and unlike the sublayers of B_6O_3#3 and B_5O_2#1, which contain messy unidirectional B-B motifs that leave the surface prone to structural deformation and further oxidation.

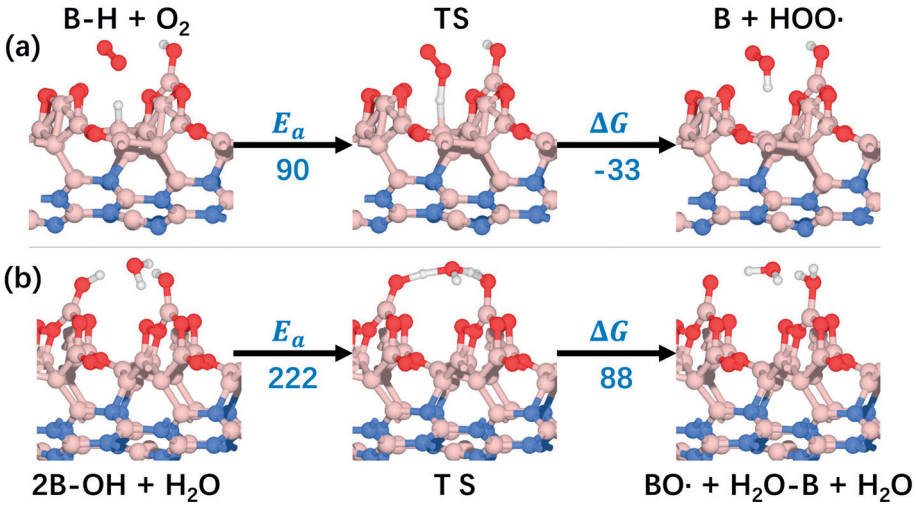

Figure 7. Structural models showing a) initiation of an HOO· radical from surface BH and gas-phase O_2, and b) regeneration of the surface BO· site from BOH species mediated by a bridging water molecule in B_6O_3#2. The activation energy and overall ΔG values (in kJ mol^{-1}) are labeled on connecting arrows. Key: boron (pink), nitrogen (blue), oxygen (red), hydrogen (white), transition state (TS).

 © 2020 Wiley-VCH Verlag GmbH & Co. KGaA, Weinheim

After determining the major active surface species and possible routes for the generation of free radicals via surface reactions, we investigated the role that surface species may have in radical quenching. We previously reported on the effect of varying catalyst mass within a given packed bed volume.[15] For a given set of reaction conditions, there is a volcano-type dependence of the reaction rate on catalyst mass, suggesting a balance between surface-derived radical generation and termination events. To test this hypothesis, we investigated interactions between the $>BO^{\bullet}$ species formed upon O_2 dissociative adsorption and gas-phase radical species. As O_2 in the gas phase is likely to interact with propyl species formed after propane activation, thereby forming $HOO^{\bullet}$ radicals (see proceeding discussion), we assessed their possible quenching reaction on the catalyst surface. The reaction of gas-phase $HOO^{\bullet}$ with a surface $>BO^{\bullet}$ species to form BOH and an O_2 molecule is described in Figure S6. This reaction is barrierless, with an overall $\Delta G = -94\ kJ\,mol^{-1}$. As such, surface quenching of radicals likely modulates the overall concentration of radicals available for gas-phase chemistry, as well as the concentration of reactive $>BO^{\bullet}$ species on the surface.

H abstraction from propane by $>BO^{\bullet}$ leads to the formation of BOH surface species that have been verified experimentally in previous investigations.[1,8,26] These sites, however, are expected to be fairly unreactive and, as such, we investigated active-site regeneration. Starting from the experimental observation that water enhances the observed reaction rate at all studied reaction conditions, we assessed the possibility of water enabling active-site regeneration. More specifically we envisioned the dehydration of two $>BOH$ sites mediated by water. In this scenario, a water molecule bridges between two BOH groups that are approximately 5 Å apart via hydrogen bonding, thereby enabling proton transfer and subsequent surface dehydration (Figure 7b). This reaction leads to the formation of a $>BO^{\bullet}$ species, and an adsorbed H_2O–B with an $E_a = 220\ kJ\,mol^{-1}$ and an overall $\Delta G = 88\ kJ\,mol^{-1}$. The newly formed water desorbs from the surface in a consecutive step with ΔG of $61\ kJ\,mol^{-1}$, and the initial {BB} site is recovered to close the catalytic cycle (Figure S8). The activation energy of this water-mediated surface-regeneration process is compatible with experimentally reported apparent activation energies for hBN-catalyzed ODH in the 200–250 $kJ\,mol^{-1}$ range.[6,12,27] Therefore, we hypothesize that this water-mediated site regeneration is the rate-limiting reaction in the overall ODH reaction, and not the H abstraction from the alkane substrate as hypothesized for vanadium.[20,28]

Summarizing the findings from our computational studies, we identified two radical initiation mechanisms Reactions (2) and (3), and Reaction (4):

$$\{BB\} + O_2 \xrightarrow{k_{init,\,O_2}} BOOB \xrightarrow{fast} 2\,BO^{\bullet} \quad (2)$$

$$\{BB\} + H_2O \xrightarrow{k_{init,\,H_2O}} BOH + BH \quad (3)$$

$$BH + O_2 \xrightarrow{fast} B^{\bullet} + HOO^{\bullet} \quad (4)$$

In addition, the high activation barrier for the water-assisted surface regeneration Reaction (5) (Figure 7b), suggests that regeneration of reactive $BO^{\bullet}$ and $B^{\bullet}$ species is rate controlling. This hypothesis is in line with the observed first-order rate dependence in water (Figure S1).

$$BOH + BOH \xrightarrow{H_2O} BO^{\bullet} + B^{\bullet} + H_2O \quad (5)$$

The radicals generated during the ODH reaction can terminate according to two pathways. First, in a radical–radical recombination Reaction (6):

$$\text{radical} + \text{radical} \rightarrow \text{non-radical products} \quad (6)$$

Or in a surface termination Reaction (7), with Figure S5 describing one predicted route:

$$>BO^{\bullet} + HOO^{\bullet} \rightarrow > BOH + O_2 \quad (7)$$

Figure 8 summarizes the key surface reactions that take place over B_6O_3#2 sites. We also note that, although only one of the candidate surface sites appears to possess the desired reactivity characteristics, there are likely more of them because our exploration of the surface reconstruction under reaction conditions is limited by the size of the model and computational expense.

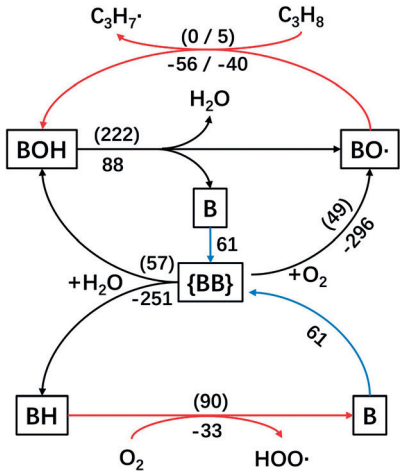

Figure 8. Reaction network diagram showing the key surface reactions on the B_6O_3#2 surface state. The energetics (in $kJ\,mol^{-1}$) of each step are labeled along the corresponding arrows, with numbers inside and outside the parentheses standing for reaction barrier and ΔG, respectively. The surface species are surrounded by black boxes. Red and blue arrows highlight the initiation of gas-phase radicals and the regeneration of the {BB} site, respectively.

The role of gas-phase chemistry on ODH performance

Building on the chemistry predicted to occur on the catalyst surface, we investigated the possible gas-phase

 © 2020 Wiley-VCH Verlag GmbH & Co. KGaA, Weinheim

reaction network. Our aim for this model was to capture the key features of boron-catalyzed ODH (that is, dehydrogenation versus cracking chemistry) with only the essential reaction network needed. As such, we focused on the first radicals formed from surface activation of propane and oxygen, which are likely critical in defining the selectivity of the ODH process. After surface activation of propane, both primary and secondary propyl radicals will react with molecular oxygen to form HOO• through a second H abstraction step (Reactions (8) and (9)). This pathway is well described in the combustion literature and stands in kinetic competition with another established reaction; namely, unimolecular C–C bond cleavage (Reactions (10)—(13)). Under our reaction conditions, we can construct a simplified set of elementary steps to describe the primary formation of propylene from *n*/*i*-propyl radicals, the activation of propane in the gas phase via generated HOO•, and the main ODH side product C_2H_4:

$$O_2 + iC_3H_7^{\bullet} \rightarrow C_3H_6 + HOO^{\bullet} \quad (8)$$

$$O_2 + nC_3H_7^{\bullet} \rightarrow C_3H_6 + HOO^{\bullet} \quad (9)$$

$$iC_3H_7^{\bullet} \rightarrow C_3H_6 + {}^{\bullet}H \quad (10)$$

$$nC_3H_7^{\bullet} \rightarrow C_3H_6 + {}^{\bullet}H \quad (11)$$

$$iC_3H_7^{\bullet} \rightarrow C_2H_4 + {}^{\bullet}CH_3 \quad (12)$$

$$nC_3H_7^{\bullet} \rightarrow C_2H_4 + {}^{\bullet}CH_3 \quad (13)$$

This well-established chemistry identifies HOO• as the predominant H abstraction agent. We used rate coefficients compiled in the NIST Chemical Kinetics Database from various sources.[29–32] The relative rate of C–H abstraction (leading to propylene) to C–C cracking (leading to ethylene) can be gauged as a function of the oxygen partial pressure by Equation (1a) (for the derivation and rate constants, see the Supporting Information):

$$\frac{R_{C_3H_6}}{R_{C_2H_4}} = \frac{([O_2](k_9 + \frac{k_8[iC_3H_7^{\bullet}]}{[nC_3H_7^{\bullet}]}) + k_{11} + \frac{k_{10}[iC_3H_7^{\bullet}]}{[nC_3H_7^{\bullet}]})}{(k_{13} + \frac{k_{12}[iC_3H_7^{\bullet}]}{[nC_3H_7^{\bullet}]})} \quad (1a)$$

While the iC_3H_7/nC_3H_7 ratio is not directly experimentally accessible, we can evaluate Equation (1a) in two limiting scenarios: 1) gas-phase activation of C_3H_8 via Reactions (14) and (15), and 2) surface activation of C_3H_8 via >BO• species formed from site B_6O_3#2 as described in Figure S4 (Reactions (16) and (17)). The rate coefficient ratio of Reactions (14) and (15) leads to $iC_3H_7/nC_3H_7 = 1.5$, reflecting the slightly higher activation barriers reported for the abstraction of primary H atoms by HOO• and the number of primary versus secondary H atoms in propane. Similarly, we used the computed barriers for the surface H abstraction by BO• to predict $iC_3H_7/nC_3H_7 = 0.74$ under scenario 2, favoring the formation of *n*-propyl radicals. This result reflects the higher reactivity of BO• species relative to HOO• radicals, which makes the surface sites less selective for secondary C–H bonds in propane.

$$C_3H_8 + HOO^{\bullet} \rightarrow iC_3H_7^{\bullet} + H_2O_2 \quad (14)$$

$$C_3H_8 + HOO^{\bullet} \rightarrow nC_3H_7^{\bullet} + H_2O_2 \quad (15)$$

$$C_3H_8 + > BO^{\bullet} \rightarrow iC_3H_7^{\bullet} + > BOH \quad (16)$$

$$C_3H_8 + > BO^{\bullet} \rightarrow nC_3H_7^{\bullet} + > BOH \quad (17)$$

With Equation (1a), we compared the estimated $R_{C_3H_6}/R_{C_2H_4}$ with the experimental ratio of C_3H_6 and C_2H_4 production rates while varying the O_2 partial pressure under different reaction conditions (Figure 9). We found that our experimental response up to 15% O_2 concentration lies between the limiting scenarios, with gas-phase propane activation overestimating (Figure 9, red line) and surface activation underestimating (Figure 9, blue line) the experimental ratios. When we varied the relative contributions of the surface and gas-phase propane H abstraction to 42% and 58% respectively, we obtained good agreement between our model-predicted $R_{C_3H_6}/R_{C_2H_4}$ ratio and the experimental observations within a broad O_2 concentration range (Figure 9, black line).

This model suggests that, under ODH conditions, there may be a mix of surface and gas-phase propane H abstraction, leading to an approximately equimolar amount of *i*- and *n*-propyl radicals being formed. The H_2O_2 formed in Reactions (14) and (15) is decomposed into water and oxygen,[17] or it can react barrierless with surface >BO• species to form additional HOO• radicals (Figure S7).

Our proposed reaction mechanism (simplified schematic depicted in Figure 10) clearly highlights the importance of

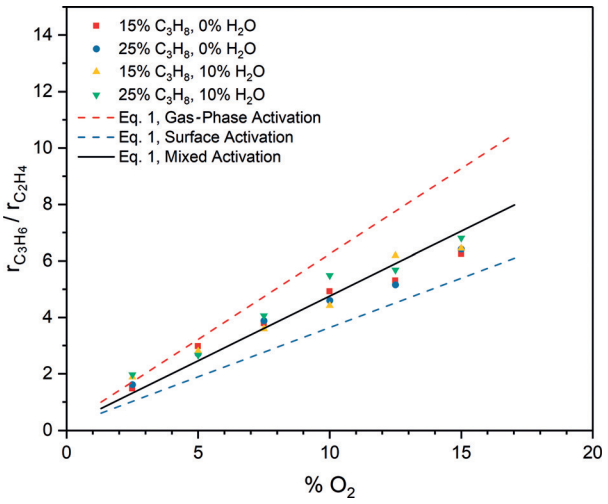

Figure 9. Comparison of experimental rates of propylene and ethylene formation as a function of O_2 concentration at $T = 525$ °C. Lines are the calculated ratio between C_3H_6 and C_2H_4 production rates derived from Equation (1) using three separate cases. Case 1 (red line): propane activation by free HOO• radicals in the gas phase, leading to a $iC_3H_7/nC_3H_7 = 1.5$. Case 2 (blue line): propane activation by surface BO• species, leading to a $iC_3H_7/nC_3H_7 = 0.74$. Case 3 (black line): mixed activation by surface species (42%) and free HOO• radicals (58%), leading to a $iC_3H_7/nC_3H_7 = 1.06$. Ratio of overall $r_{C_3H_6}/r_{C_2H_4}$ based on experimental rates of formation of propylene and ethylene. Propane conversions were kept below 5% under all conditions to approximate differential conditions.

 © 2020 Wiley-VCH Verlag GmbH & Co. KGaA, Weinheim

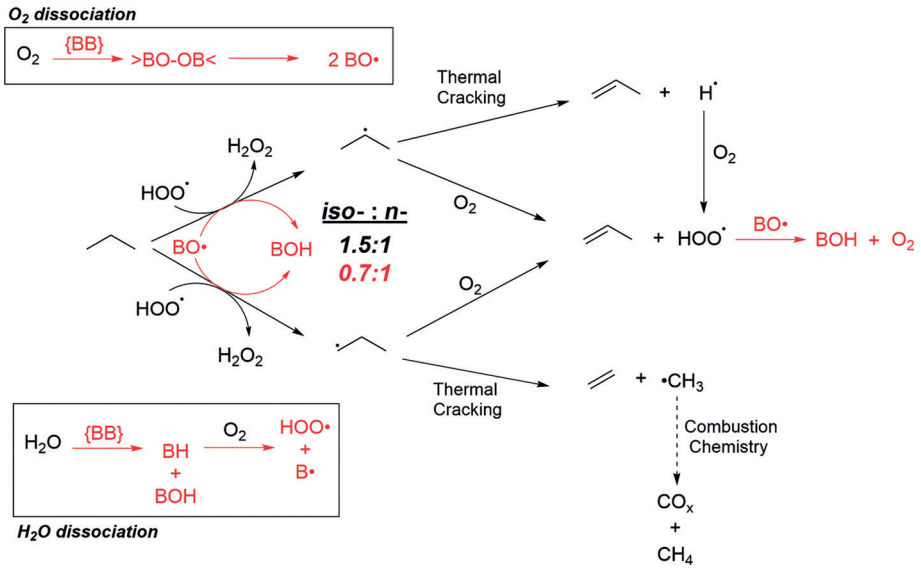

Figure 10. Simplified reaction network describing the key reactions involved in the combined surface (red-colored) and gas-phase (black-colored) ODH of propane to propylene and ethylene; iso-:n- ratios shown in the Figure detail the propyl radical distribution of gas-phase and surface propane H abstraction. Overoxidation of methyl radicals is expected to follow conventional combustion chemistry routes to form methane and carbon oxides, while at high conversions overoxidation of propylene may lead to additional CO_x formation. H_2O_2 can decompose to form water in the gas phase or HOO• on the catalyst surface, as discussed in the text.

free-radical gas-phase chemistry as well as surface-mediated reactions in explaining catalyst performance. This simple model is, to our knowledge, the first mechanistic hypothesis that can predict the experimentally observed product distribution of BO_x-catalyzed ODH over a range of oxygen partial pressures.

According to this simple model, propane is consumed in Reactions (14)–(17), leading to the expression Equation (2a) for the propane consumption:

$$\frac{d[C_3H_8]}{dt} = (k_{14} + k_{15})[HOO^{\bullet}][C_3H_8] + (k_{16} + k_{17})[>BO^{\bullet}][C_3H_8] \quad (2a)$$

We point out that both HOO• and >BO• can either propagate upon reaction with propane or terminate (Reactions (6) and (7)). This leads to a higher radical quasi steady-state concentration—at a given conversion—at higher propane concentrations, leading to the apparent second order observed for propane (Figure 1).

From a catalytic materials perspective, we hypothesize that surface species that can initiate oxidation while also favoring *i*-propyl radical formation would lead to enhanced ODH performance. Indeed, the formation of *n*-propyl radicals inevitably leads to non-negligible formation of C–C cracking products. On the other hand, the more favorable iC_3H_7/nC_3H_7 distribution stemming from gas-phase propane H abstraction suggests that optimizing the void space in a catalyst bed, as well as the development of catalysts that can generate HOO• radicals rather than alkyl radicals, may provide additional benefits during ODH.

Conclusion

The combined surface and gas-phase reaction network reported herein provides a sound mechanistic framework for future studies of boron-containing materials. While upon first inspection the addition of a gas-phase may prove complex, we have shown that it is the gas-phase component itself that enables the outstanding product distribution observed with boron-based catalysts. This situation, where the surface initiates a free-radical gas-phase reaction, stands in sharp contrast with the mechanisms that have been proposed in the literature for vanadium-based catalysts. Indeed, those systems operate via a Mars van Krevelen mechanism where oxidized vanadium species presumably homolytically activate a C–H bond of propane.[33] Although never observed experimentally, the nascent radicals are assumed to remain adsorbed to the surface and react consecutively with propylene via a second H abstraction (so-called rebound mechanism), leaving behind a reduced vanadium surface site. Reoxidation of the surface with oxygen to regenerate the H-abstracting species is fast and not rate-determining, explaining the zero-order kinetics in oxygen.[20]

Contrasting this reaction mechanism with the one proposed for boron catalysts, there are two major differences. For the boron-initiated mechanism, a key role of the catalyst is to generate the reactive species (HOO• radicals) that activate the propane substrate in the gas phase, leading to fast radical propagation. A fraction of the propane reacts directly with the catalyst surface during chain initiation, playing a critical role in establishing the distribution of available propyl species in the gas phase. This reaction channel in turn lights off a gas-phase reaction and leads to the oxyfunctionalization of the BN surface under ODH conditions. We emphasize that heating BN in the presence of oxygen only does not result

 © 2020 Wiley-VCH Verlag GmbH & Co. KGaA, Weinheim

in surface oxidation, implying that the oxyfunctionalization goes hand-in-hand with the gas-phase radical chemistry. Our computational studies also highlight the complexity of this oxidation, leading to a variety of boron species with different reactivities. In contrast, the well-studied vanadium-based catalysts are assumed to primarily activate the C–H bond of propane at the surface. This, in combination with stronger interactions of the reaction intermediates with the catalyst surface, and potentially the propylene product, explains the rapid loss in selectivity as the propane conversion increases for vanadium-based catalysts.

We conclude that optimal ODH catalysts should 1) generate reactive H-abstracting species that favor the abstraction of secondary C–H bonds in propane, and 2) not interact strongly with intermediates and products to minimize fast consecutive surface oxidation steps. These conclusions are in line with studies by Iglesia et al. exploring $^{\bullet}$OH-mediated oxidation of methane,[34] and Deshlahra et al. investigating NO_x-mediated ODH reactions;[35] moreover, they reveal a general set of guidelines with which to pursue development of more selective catalysts.

Acknowledgements

The authors acknowledge the financial support of the U.S. Department of Energy, Office of Science, Office of Basic Energy Sciences, under award DE-SC0017918 (reactivity studies and material characterization), and DOE-BES Award DE-SC0019152 (computational studies), and utilized resources of the National Energy Research Scientific Computing Center (NERSC), a U.S. Department of Energy (DOE) Office of Science User Facility operated under Contract No. DE-AC02-05CH11231.

Conflict of interest

The authors declare no conflict of interest.

Keywords: boron nitride · boron oxide · radical chemistry · surface oxidation · water promotion

[1] J. M. Venegas, W. P. McDermott, I. Hermans, *Acc. Chem. Res.* **2018**, *51*, 2556 – 2564.
[2] J. Tian, J. Lin, M. Xu, S. Wan, J. Lin, Y. Wang, *Chem. Eng. Sci.* **2018**, *186*, 142 – 151.
[3] L. Shi, Y. Wang, B. Yan, W. Song, D. Shao, A.-H. Lu, *Chem. Commun.* **2018**, https://doi.org/10.1039/C8CC04604B.
[4] R. Huang, B. Zhang, J. Wang, K.-H. Wu, W. Shi, Y. Zhang, Y. Liu, A. Zheng, R. Schlögl, D. S. Su, *ChemCatChem* **2017**, *9*, 3293 – 3297.
[5] J. T. Grant, C. A. Carrero, F. Goeltl, J. Venegas, P. Mueller, S. P. Burt, S. E. Specht, W. P. McDermott, A. Chieregato, I. Hermans, *Science* **2016**, *354*, 1570 – 1573.
[6] P. Chaturbedy, M. Ahamed, M. Eswaramoorthy, *ACS Omega* **2018**, *3*, 369 – 374.
[7] A. M. Love, B. Thomas, S. E. Specht, M. P. Hanrahan, J. M. Venegas, S. P. Burt, J. T. Grant, M. C. Cendejas, W. P. McDermott, A. J. Rossini, I. Hermans, *J. Am. Chem. Soc.* **2019**, *141*, 182 – 190.
[8] A. M. Love, M. C. Cendejas, B. Thomas, W. P. McDermott, P. Uchupalanun, C. Kruszynski, S. P. Burt, T. Agbi, A. J. Rossini, I. Hermans, *J. Phys. Chem. C* **2019**, *123*, 27000 – 27011.
[9] Z. Zhang, E. Jimenez-Izal, I. Hermans, A. N. Alexandrova, *J. Phys. Chem. Lett.* **2019**, *10*, 20 – 25.
[10] W.-D. Lu, D. Wang, Z. Zhao, W. Song, W.-C. Li, A.-H. Lu, *ACS Catal.* **2019**, *9*, 8263 – 8270.
[11] J. M. Venegas, J. T. Grant, W. P. McDermott, S. P. Burt, J. Micka, C. A. Carrero, I. Hermans, *ChemCatChem* **2017**, *9*, 2118 – 2127.
[12] L. Shi, B. Yan, D. Shao, F. Jiang, D. Wang, A.-H. Lu, *Chin. J. Catal.* **2017**, *38*, 389 – 395.
[13] N. R. Altvater, R. W. Dorn, M. C. Cendejas, W. P. McDermott, B. Thomas, A. J. Rossini, I. Hermans, *Angew. Chem. Int. Ed.* **2020**, *59*, 6546 – 6550; *Angew. Chem.* **2020**, *132*, 6608 – 6612.
[14] W. P. McDermott, J. Venegas, I. Hermans, *ChemSusChem* **2020**, *13*, 152 – 158.
[15] J. M. Venegas, I. Hermans, *Org. Process Res. Dev.* **2018**, *22*, 1644 – 1652.
[16] E. Spier, U. Neuenschwander, I. Hermans, *Angew. Chem. Int. Ed.* **2013**, *52*, 1581 – 1585; *Angew. Chem.* **2013**, *125*, 1622 – 1626.
[17] X. Zhang, R. You, Z. Wei, X. Jiang, J. Yang, Y. Pan, P. Wu, Q. Jia, Z. Bao, L. Bai, M. Jin, B. Sumpter, V. Fung, W. Huang, Z. Wu, *Angew. Chem. Int. Ed.* **2020**, *59*, 8042 – 8046; *Angew. Chem.* **2020**, *132*, 8119 – 8123.
[18] K. Takanabe, E. Iglesia, *J. Phys. Chem. C* **2009**, *113*, 10131 – 10145.
[19] K. Takanabe, S. Shahid, *AIChE J.* **2017**, *63*, 105 – 110.
[20] K. Chen, A. Khodakov, J. Yang, A. T. Bell, E. Iglesia, *J. Catal.* **1999**, *186*, 325 – 333.
[21] S. T. Oyama, A. M. Middlebrook, G. A. Somorjai, *J. Phys. Chem.* **1990**, *94*, 5029 – 5033.
[22] L. Leveles, K. Seshan, J. A. Lercher, L. Lefferts, *J. Catal.* **2003**, *218*, 296 – 306.
[23] Z. Zhang, B. Zandkarimi, A. N. Alexandrova, *Acc. Chem. Res.* **2020**, *53*, 447 – 458.
[24] H. Zhai, A. N. Alexandrova, *ACS Catal.* **2017**, *7*, 1905 – 1911.
[25] L. M. Aparicio, S. A. Rossini, D. G. Sanfilippo, J. E. Rekoske, A. A. Trevino, J. A. Dumesic, *Ind. Eng. Chem. Res.* **1991**, *30*, 2114 – 2123.
[26] J. T. Grant, W. P. McDermott, J. M. Venegas, S. P. Burt, J. Micka, S. P. Phivilay, C. A. Carrero, I. Hermans, *ChemCatChem* **2017**, *9*, 3623 – 3626.
[27] J. Tian, J. Tan, M. Xu, Z. Zhang, S. Wan, S. Wang, J. Lin, Y. Wang, *Sci. Adv.* **2019**, *5*, eaav8063.
[28] C. A. Carrero, R. Schlögl, I. E. Wachs, R. Schomaecker, *ACS Catal.* **2014**, *4*, 3357 – 3380.
[29] H. J. Curran, *Int. J. Chem. Kinet.* **2006**, *38*, 250 – 275.
[30] R. S. Konar, R. M. Marshall, J. H. Purnell, *Trans. Faraday Soc.* **1968**, *64*, 405.
[31] J. Warnatz, *Combustion Chemistry*, Springer New York, New York, **1984**, pp. 197 – 360.
[32] W. Tsang, *J. Phys. Chem. Ref. Data* **1988**, *17*, 887 – 951.
[33] X. Rozanska, R. Fortrie, J. Sauer, *J. Phys. Chem. C* **2007**, *111*, 6041 – 6050.
[34] K. Takanabe, E. Iglesia, *Angew. Chem. Int. Ed.* **2008**, *47*, 7689 – 7693; *Angew. Chem.* **2008**, *120*, 7803 – 7807.
[35] L. Annamalai, Y. Liu, P. Deshlahra, *ACS Catal.* **2019**, *9*, 10324 – 10338.

Manuscript received: March 11, 2020
Revised manuscript received: May 26, 2020
Accepted manuscript online: June 22, 2020
Version of record online: July 14, 2020

 © 2020 Wiley-VCH Verlag GmbH & Co. KGaA, Weinheim